韓國鑛物學會誌 第 7 卷 第 1 號(1994)
J. Miner. Soc. Korea, 7, 49－61(1994)

Formation of Clay Minerals by Water-Rock Interaction in the Fracture of Gneiss

편마암 열극에서의 물-암석 상호반응에 의한 점토광물 생성

Chan Ho Jeong (정찬호)* · Soo Jin Kim (김수진)** · Yong Kwon Koh (고용권)*

*Korea Atomic Energy Research Institute, Taejeon 305-606, Korea
(한국원자력연구소)
**Department of Geological Sciences, Seoul National University, Seoul 151-742, Korea
(서울대학교 지질과학과)

ABSTRACT : As the groundwater flows along the fractures of crystalline rocks, it will be in contact with the fracture walls mostly coated by secondary minerals which are quite different from those of host rocks. The presence of fracture-filling minerals in crystalline rocks is important on the view point of radioactive waste disposal because of their great surface reactivity. The Surichi drill hole of 200 m in depth in the Yugu area composed mainly of Precambrian gneiss was selected to study the formation process of clay minerals on the fracture wall of gneiss, and their relation with present groundwater.

The water-rock interaction in fractures resulted in the formation of gibbsite and clay minerals. They are formed by two different processes: (1) Incongruent dissolution of feldspar by groundwater diffused from a fracture path into rock matrix produced smectite and illite in situ, (2) On the wall of fracture, gibbsite, kaolinite, smectite and illite are formed by precipitation of dissolved species in groundwater. They show the paragenetic sequence such as gibbsite→kaolinite→smectite or illite. The paragenetic sequence of fracture-filling minerals was controlled by increase of pH of groundwater, decrease of fracture permeability by precipitation of fillings, and immobility of alkali or alkaline earths in groundwater.

The groundwater from the Surichi borehole is a Na-HCO_3 type with pH range of 8.6-9.2. The sodium and bicarbonate in groundwater would be supplied by the dissolution of albite and calcite, respectively. The saturation index of groundwater and surface water calculated by WATEQ4F indicates that gibbsite and kaolinite are under precipitation to equilibrium state, and that smectite and illite are under equilibrium to redissolution environment. The stability relation of clay minerals in the Na_2O-Al_2O_3-SiO_2-H_2O system shows that kaolinite is stable for all waters.

요약 : 결정질암반중의 지하수 이동로인 열극은 모암과는 다른 이차광물로 구성되는 수가 많다. 그래서 방사성폐기물 처분장 모암중의 열극광물은 그들의 높은 표면 반응성 때문에 관심의 대상이 되고 있다. 본 논문에서는 선캠브리아기 편마암류로 구성되어 있는 충남 유구지역 수리치 시추공 코아의 열극표면에서 발견된 점토광물의 생성과정을 고찰하였고, 그들과 현재 지표수 및 지하수와의 평형관계를 알아보았다.

편마암 열극에서 물－암석 상호반응은 깁사이트, 캐올리나이트, 스멕타이드, 일라이트 등을 생성시켰다. 열극점토광물은 두가지 다른 과정을 통해 생성된 것으로 판단된다 : (1) 열극주변 모암 확산대에서 장석의 Incongruent Dissolution에 의한 스멕타이트 또는 일라이트의 생성, (2) 열극틈 사이에는 깁사이트, 캐올리나이트, 스멕타이트(또는 일라이트)가 지하수의 용존이온으로부터 침전. 열극충전광물은 깁사이트→캐올리나이트→스멕타이트(또는 일라이트) 순으로의 광

물생성순서를 보인다. 광물생성순서를 규제한 요인은 지하수의 pH 상승, 충전물에 의한 열극틈의 투수계수 감소, 그리고 알카리 및 알카리토 원소의 Immobility에 의한 것으로 보인다.

수리치 시추공 지하수의 pH는 8.6-9.2 범위이며, 화학성분상 Na-HCO_3 형이며, Na와 HCO_3는 Albite와 Calcite의 용해작용으로부터 공급된 것으로 보인다. WATEQ4F 프로그램에 의한 지하수의 포화지수는 pH 상승에 따라 깁사이트와 캐올리나이트는 침전반응을 거쳐 평형상태로, 스멕타이트와 일라이트 평형상태를 거쳐 재용해성 환경으로의 변화를 지시한다. Na_2O-Al_2O_3-SiO_2-H_2O계의 상안정도상에 지표수와 지하수 모두 캐올리나이트 안정영역에 속한다.

INTRODUCTION

The rock types assumed to be potential radioactive waste repositories are crystalline rocks such as granite and gneiss. The disposed waste forms in these rocks may be subjected to groundwater attack. The corroding and leaching action of groundwater will mobilize the radionuclides which will in turn migrate and diffuse through the near- and far-field possibly reaching to biosphere. Far-field transport in the crystalline rocks is dominated and controlled by fracture system (Muller et al., 1992).

As the groundwater is transported along the fractures of crystalline rock, it will be in contact with the fissure walls which are mostly coated by secondary minerals different from those in host rock itself (Tullborg and Larson, 1982). Thus, the coating and filling minerals in fractures are of fundamental interest, particularly in respect of water-rock interaction because of their great surface reactivity (Muller et al., 1992). The fracture-filling minerals of Sweden hard rocks for radioactive waste disposal were studied by Tullborg and Larson (1982, 1983) and Tullborg (1986).

This study is part of a water-rock interaction program connected to the research project for radioactive waste disposal. The Yugu site situated approximately 50 km northeast of Taejeon has been chosen for this purpose (Fig. 1). The study site is mainly composed of Precambrian gneisses which are called "Yugu gneiss". Three holes of 50 m deep and one hole of 200 m deep had been drilled at the discharge valley ("Surichi" in the local name) in the study site. This study focuses on the borehole of 200 m in depth.

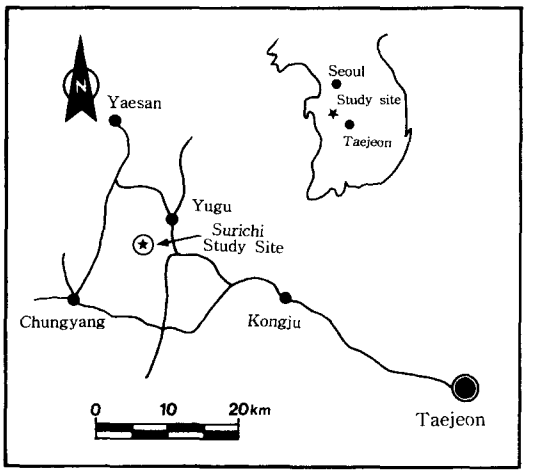

Fig. 1. Location map of the study site.

The purpose of this paper is to find out what minerals appear on the fracture walls in gneiss, at what conditions clay minerals were formed, and their relation to the water present. The results of this study can be applied to the assessment of the gneiss properties as one of possible the natural barrier function to a repository.

METHODS OF THE STUDY

Some samples of host rock and fracture-filling minerals were taken from borehole cores of 200 m in depth. The thin sections of host rock samples containing a fracture were prepared for the microscopic observation and electron microprobe analysis (EPMA). X-ray diffraction (XRD) analysis for the identification of clay minerals was made using the RIGAKU model RAD-3D diffractometer with Ni-filtered CuKα radiation. Scanning electron microscope with EDS system (JEOL model JAX-733 SEM) was applied to ob-

tain the microscopic information on fracture-fillings and weathered feldspars including dissolution of feldspars, growth of secondary minerals, and paragenetic relations of fracture-filling clay minerals. The chemical composition of feldspar was obtained by JEOL model JAX-733 eletron microprobe analyzer.

The five groundwater samples were zonally collected from the borehole of 200 m in depth. Three surface waters were obtained from a creek adjacent to the borehole. The pH, Eh, electrical conductivity and temperature of all water samples were measured in situ. Bicarbonate of water samples was measured by acid titiration using methyle orange indicator. The anions of water samples were analysed by ion chromatography (Dyonex 4500i) in the laboratory. The water samples for cation analysis were acidified with 2 drops of nitric acid (Sasowsky and White, 1993).

The cations of water samples were determined by atomic asorption spectrometer (Perkin Elmer 3100). Ion balance error of waters was examined to know the reliability of data. The analysed samples show imbalance errors within ±5 %.

The speciation and saturation index of waters with respect to mineral phases were calculated by computer program WATEQ4F (Ball and Nordstrom, 1991).

HOST ROCK

The rock type of the study site is dominated by Precambrian gneiss named "Yugu gneiss", which belongs to Kyounggi gneiss complex. It is medium- to coarse-grained massive biotite granitic gneiss. It shows locally banded or augen gneiss. The lithology of the borehole core is shown in Fig. 2. Calcite and quartz veins are abundantly found in the gneiss. Fault clays and breccias, and slickensides are frequently found in fractured zones and faults in small scale. At 195 m in depth, the gneiss is cut by a felsic dyke of 2 m thick. Much of the rocks were subjected to hydrothermal alteration more than 127 million years ago (So et al., 1988). The strike of foliation of gneiss is N15° W-N80° E and its dip is 35-75°.

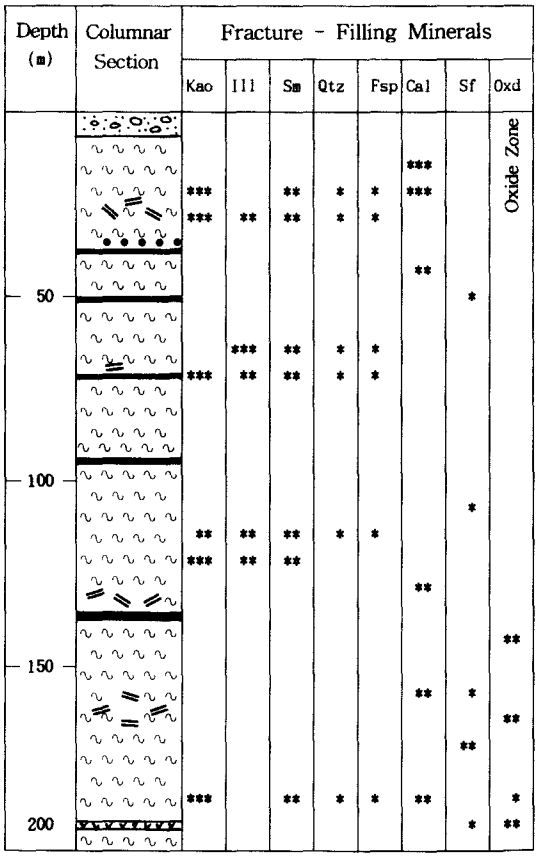

Fig. 2. Lithology and fracture-filling minerals of the borehole core in the Surichi site.

Note: Kao;Kaolinite, Ill;Illite, Sm;Smectite, Qtz; Quartz, Fsp;Feldspar, Cal;Calcite, Sf;Sulfide, Oxd;Fe- or Mn-Oxide.
***:Abundant, **:Common, *:A little.
:Alluvium :Gneiss :Dyke
:Quartz & Calcite Vein
:Pyrite enrichment zone
:Fault with slickenside or fault clays

Minerals

The major minerals of gneiss are quartz, K-feldspar, plagioclase, biotite and muscovite, and

Table 1. Chemical analysis of feldspars by EPMA.

	1	2	3	4	5	6	7
SiO_2	66.67	60.87	64.80	61.24	68.01	66.50	65.98
Al_2O_3	18.13	24.53	18.92	23.94	20.03	21.59	20.98
*FeO	0.25	0.01	0.20	0.01	0.01	0.07	0.45
MnO	0.02	0.03	0.06	0.04	0.06	0.02	0.03
MgO	0.01	—	0.01	—	—	—	0.08
CaO	—	5.75	0.20	5.27	0.20	1.53	0.76
Na_2O	0.11	8.58	3.13	8.99	11.60	10.74	10.02
K_2O	14.60	0.30	11.77	0.07	0.03	0.37	1.90
Total	99.79	100.07	99.09	99.56	100.00	100.53	100.21
	Numbers of cations on the basis of 32 oxygen						
Si	12.046	10.829	11.911	10.926	11.890	11.604	11.644
Al	4.042	5.144	4.098	5.034	4.127	4.441	4.364
Fe	0.039	0.002	0.031	0.001	0.001	0.010	0.066
Mn	0.004	0.004	0.009	0.007	0.008	0.002	0.005
Mg	0.004	—	0.003	—	—	—	0.021
Ca	—	1.096	0.040	1.008	0.038	0.287	0.144
Na	0.039	2.959	1.114	3.112	3.931	3.634	3.429
K	3.523	0.062	2.760	0.017	0.008	0.008	0.427
Mole (%)							
Or	98.9	1.5	70.5	0.4	0.1	0.2	10.7
Ab	1.1	71.9	28.5	75.2	98.9	92.5	85.7
An	—	26.6	1.0	24.4	1.0	7.3	3.6

* Iron is total Fe.

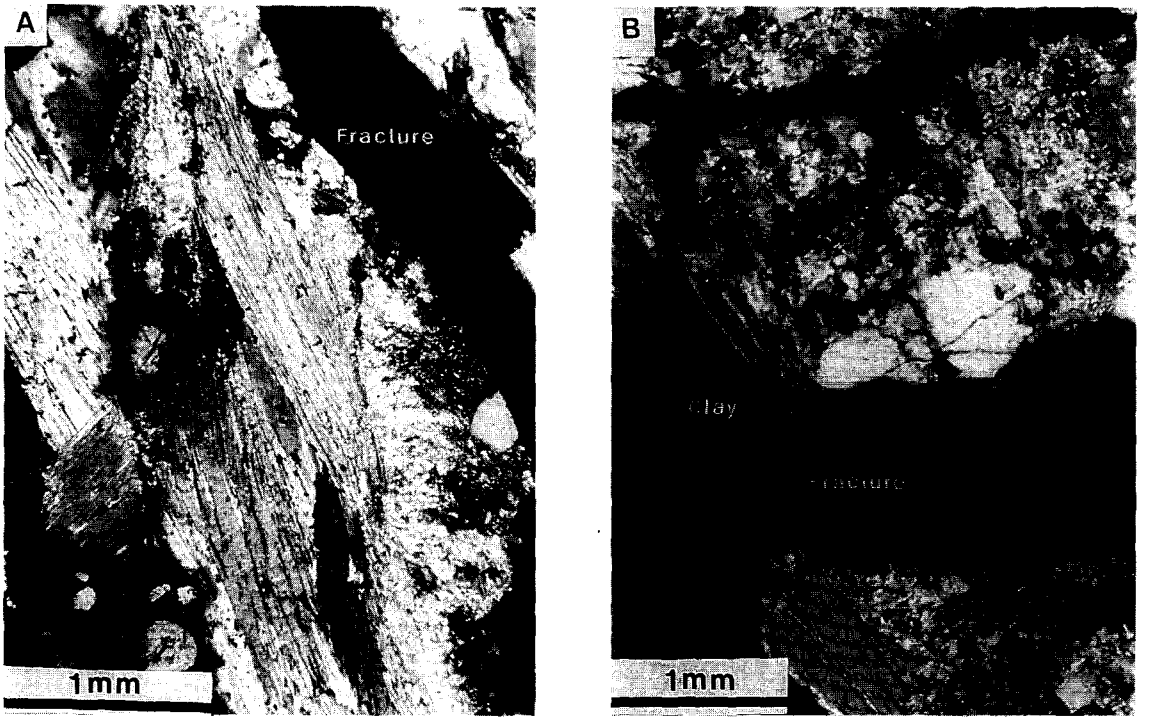

Fig. 3. Photomicrographs showing the alteration of gneiss and fracture wall-coatings in gneiss (A : Sericitization of feldspar and chloritization along basal cleavage of biotite, B : milky clays lining along fracture wall of gneiss).

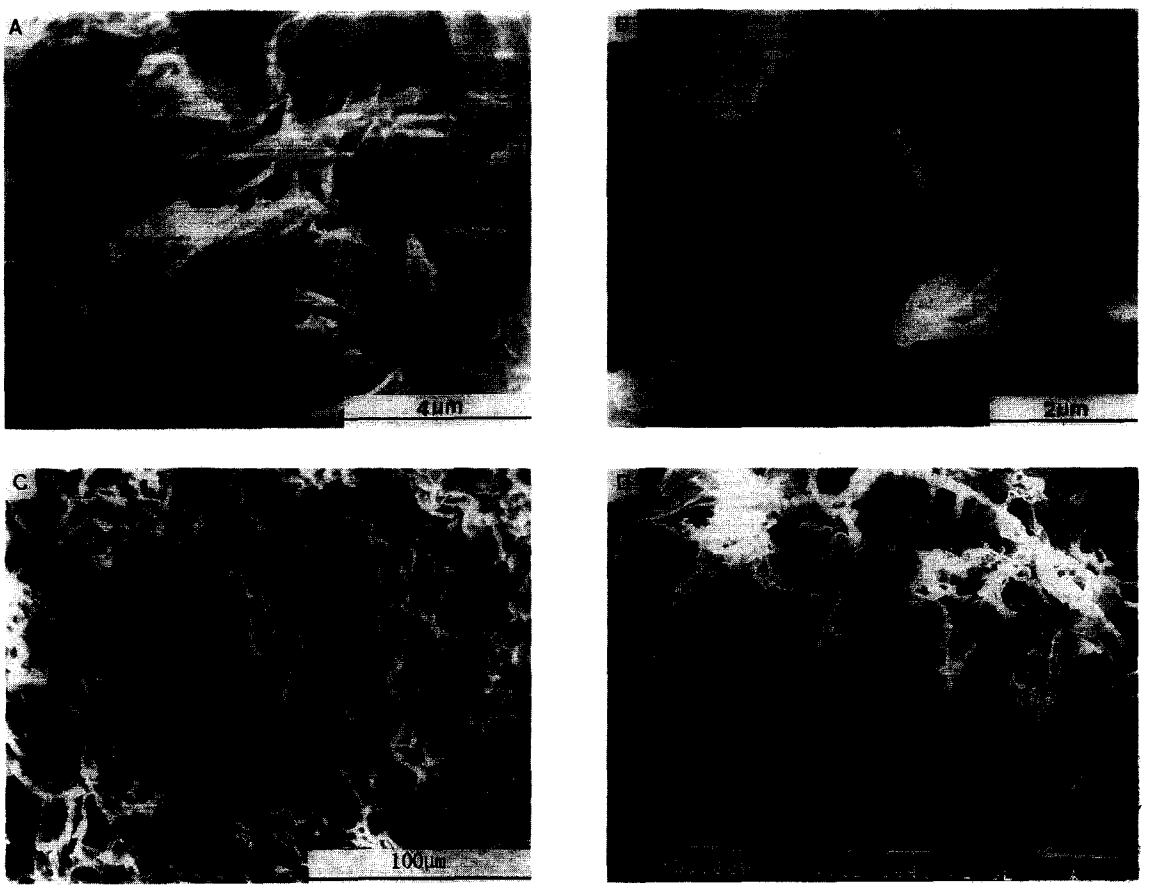

Fig. 4. SEM micrographs showing the weathering of feldspars in the rock matrix. A : Smectite and illite altered from plagioclase, B : Etch pits of plagioclase and curling smectite on feldsapr, C : Rectangular breakdown of K-feldspar and precipitation of smectite, D : Honeycomb smectite altered from plagioclase.

its minor constituents are calcite, monazite, zircon, pyrite and opaque minerals. The major primary minerals such as mica and feldspar were mostly altered to sericite and chlorite (Fig. 3).

Some whitish spots observed in the rock matrix turns out that some feldspar around fractures are weathered into clay minerals. The clays altered from feldspars were identified as smectite and illite by X-ray diffraction analysis (Fig. 6). The chemical compositions of feldspars are given in the Table 1. Most of plagioclases belong to albite and oligoclase of Ab_{98-72} in chemical composition. K-feldspar having Or_{99-71} is occasionally found in the gneiss.

FRACTURE-FILLING MINERALS

The frequent fracture-filling materials gibbsite, kaolinite, smectite, illite, pyrite, chalcopyrite, quartz, feldspar, and Fe- or Mn-oxides. The fracture-fillings from core samples of the borehole were summarized in Fig. 2.

Clay Minerals

Clay minerals occur as whitish fracture wall-coatings in core samples (Fig. 5A). Under the microscope, clays occur as linings along the fracture in gneiss (Fig. 3B). Their XRD patterns show

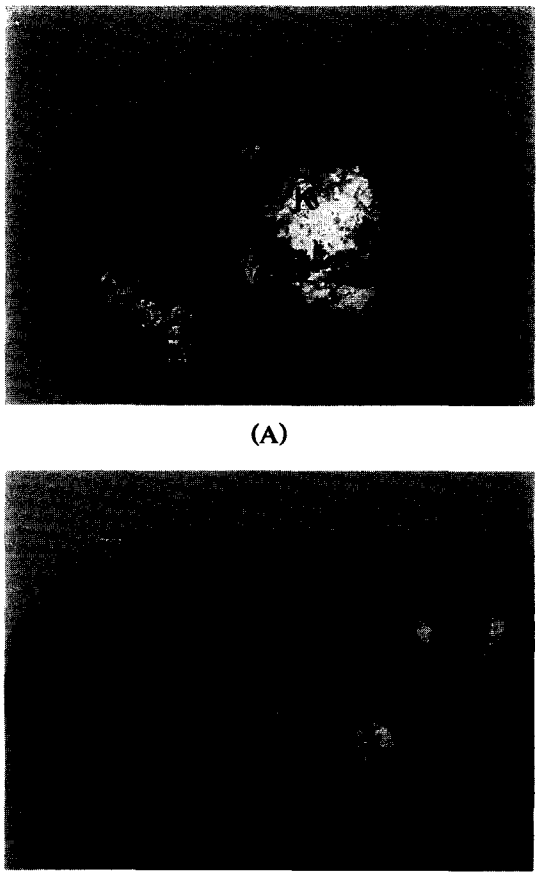

Fig. 5. Photographs showing coatings on open fracture walls of geneiss cores. A : Fracture-coating whitish clays (K) B : Acicular and platy calcites on the fracture wall. The diameter of rock cores is 5.5 cm.

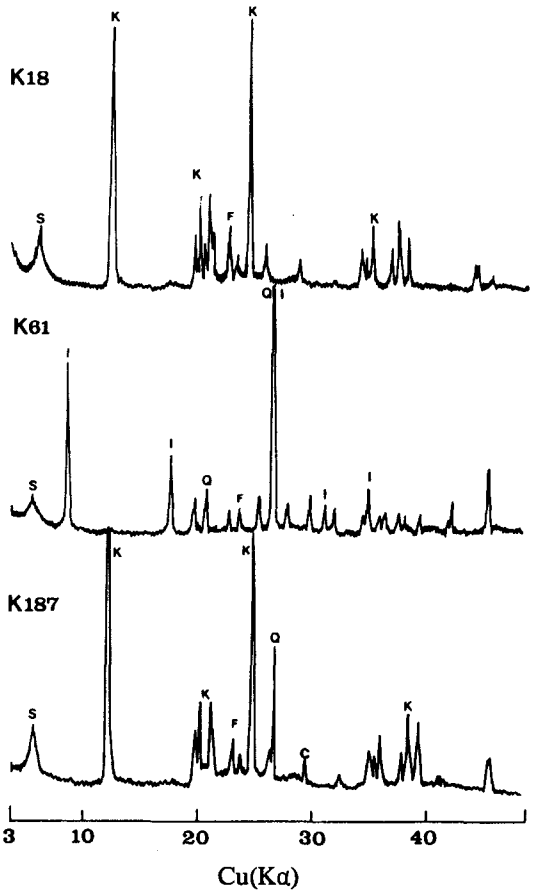

Fig. 6. X-ray diffraction patterns of secondary clay minerals in the fracture of gneiss cores (S : smectite, K : kaolinite, I : illite, Q : quartz, F : feldspar, C : calcite).

kaolinite as dominant constituent, whereas smectite and illite as minor clay minerals (Fig. 6). Smectite and illite assemblage occurs as weathering pro-ducts of feldspar in rock matrix.

The basal reflection of some smectite under natural humidity condition in the core shows 19-20 Å swelling state. Smectite dried at room temperature for a week shows basal reflection of about 15 Å. It means that smectitic clay was saturated with groundwater in the fracture. Smectite occurs as the curling leaves on kaolinite crystals under the scanning electron microscope (Fig. 7).

Kaolinite shows large pseudohexagonal cysals of more than 2 ㎛ in thickness and 10 ㎛ in length. As shown in Fig. 7, some kaolinite has book-structure. The basal reflections 7.17 Å(001) and 3.57 Å(002) of kaolinite is shown in Fig. 6. Growth of a large kaolinite may require both physically and chemically stable environment which continue for a long time as suggested by Keller (1977). In the crystalline rocks, the soluble species formed from the feldspar was used for the growth of larger and structurally ordered kaolinite in a steady state. Such condition can be expected in the fracture flow paths of crystalline rocks which show sluggish flow rate.

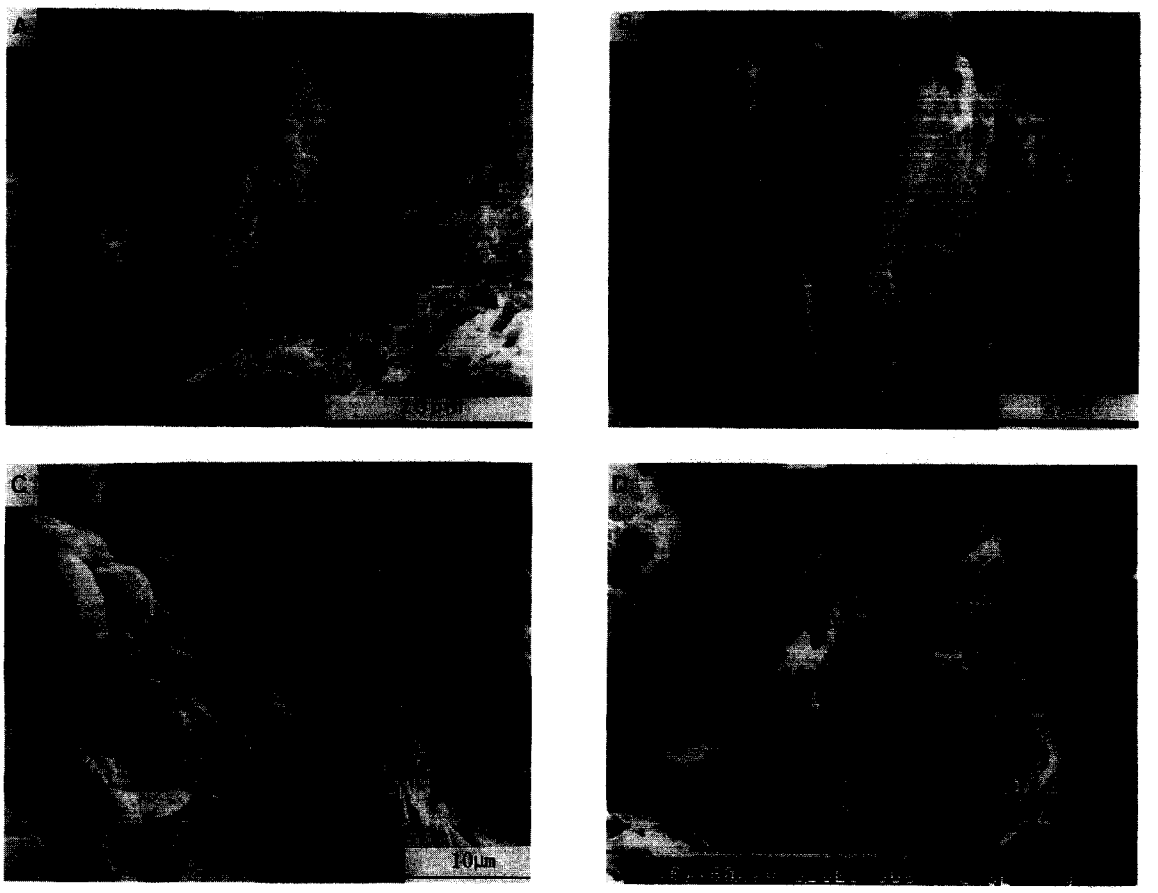

Fig. 7. SEM micrographs showing the fracture-filling clay minerals A : Overgrowth of smectite on the kaolinite crystals on the fracture wall, B : Curling smectite overgrowing on layer staked kaolintes, C : Pseudohexagonal kaolinite assemblages in fracture, D : Smectite(or illite) overgrown on the kaolinite assemblages on fracture wall.

Illite is $2M_1$ type showing maximum reflection of 10.04 Å(002) and 3.34 Å(006) in XRD patterns. The formation of clay minerals by weathering of feldspar is shown in Fig. 4. Illite shows a hair-like morphology. It always occurs together with smectite. Thus, they are not easily discerned under scanning electrom microscope without EDS image (Fig. 4).

Other Minerals

Gibbsite is occasionally found as whitish soft coatings on the fracture walls. Most of the Fe-oxides present as fracture fillings are iron oxyhydroxide (FeOOH). Pyrite (FeS_2), and chalcopyrite ($CuFeS_2$) are frequently found. Both minerals occur as thin platy particles. The iron oxyhydroxide occurs like film coatings on the fracture wall from surface to 29 m deep (Fig. 2). Calcite is ubiquitous in fracture walls of the core samples. The platy friable calcites are found in fracture (Fig. 5B).

FORMATION OF CLAY MINERALS IN THE FRACTURE

In the fractured rock mass, water-rock interaction is possibly restricted to a rather narrow area

along the fractures. The reactions taking place in the fracture are dissolution of pre-existing minerals and precipitation of secondary minerals. In the crystatlline rocks, feldspar in the host rock along the fracture flow paths is easily dissolved by the attack of H^+ in advecting groundwater.

The dissolution of feldspars present in fractures results in the formation of secondary clay minerals through two different processes : (1) In situ incongruent precipitaion, and (2) the transportation of dissolved species into fractures and the precipitation on the fracture wall. The first process leads to the formation of smectite and illite in narrow area of rock matrix along fracture. The second process results in the formation of gibbsite, kaolinite and smectite on the fracture wall. Fig. 8. is the schematic sketch showing the distribution of weathered feldspar in rock matrix along fracture and fracture-filling mineals.

The dissolution of plagioclase undergoes the reaction which can be expressed as follows :

$$\text{Plagioclase} + H^+ + H_2O \longrightarrow Na^+ + Ca^{2+} + H_4SiO_4 + Al(OH)_3 \quad (1)$$
(gibbsite)

The dissolved cations liberated from plagioclases are Ca^{2+}, Na^+, K^+, H_4SiO_4 and soluble Al species. Some dissolved chemical species are transported into fractures. Gibbsite can be formed from $Al(OH)_3$ of soluble Al species liberated from feldspar in the early precipitation stage. Gibbsite occurs as whitish soft cream form on the fracture wall. Kaolinite on the wall of fracture can be formed according to following reaction :

$$2H_4SiO_4 + 2Al(OH)_3 \longrightarrow Al_2Si_2O_5(OH)_4 + 3H_2O + 2H^+ \quad (2)$$
(kaolinite)

Kaolinite formed by above reaction is abundanly found on the fracture wall. The remarkable point among the fracture-filling clay minerals is that smectite has been overgrown on kaolinte

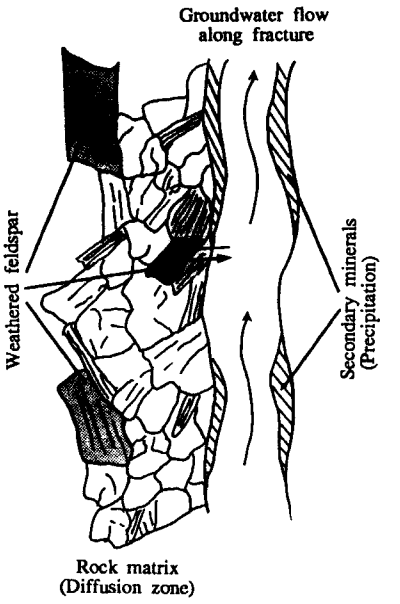

Fig. 8. Schematic sketch showing the distribution of weathered feldspar in rock matrix along fracture and fracture-filling minerals.

crystals. The paragenetic relation of the clay minerals is clearly shown under the scanning electron microscope (Fig. 7). The kaolinite-smectite paragenetic relation may be controlled by the change of groundwater chemistry and the permeability of fracture apertures.

The solute concentration and pH of groundwater increase with the precipitation of kaolinite from the dissolved solution of feldspars since H^+ is consumed continuously for dissolution of feldspar, and the dissolved chemical species are released continuously into solutions. And, continuous precipitation of kaolinites on the fracture wall results in the decrease of fracture permeability, which is called "sealing effect".

These changes give the favorable condition for the precipitation of smectite, because smectite is formed under the poorly-drained condition, high pH, and high activities of alkali and alkaline earths in groundwater. Accordingly, it is expectable that the smectite overgrows on the kaolinite

crystals formed previously on the fracture walls at late stage of precipitation.

On the thermodynamic viewpoint, smectite is much more stable than kaolinite. Gibbs free energies of formation of gibbsite, kaolinite and smectite at 25 ℃ are known as -276.1 kcal/mol, -902.9 to 905.7 kcal/mol and -2.579.6 kcal/mole, respectively (Anovitz et al, 1991; Huang and Keller, 1973; Nriagu, 1975; Wood and Garrels, 1987). The pre-cipitation sequences from incongruent dissolution of feldspar is gibbsite, kaolinite, and smectite in order on the thermodynamic viewpoint. The formation sequences of clay minerals on the fracture wall in the gneiss are consistent with thermodynamic precipitation sequences.

However, the formation of clay minerals in rock matrix attributed to the process different from the formation of fracture-filling clays. Some feldspars in the gneiss matrix along the fractures are weathered into clay minerals, which are usually found as whitish spots. Under the microscope, the weathered feldspars show dissolution and breakdown textures such as etch pits and rectangular discrepancy on the surface (Fig. 4).

The alteration products of feldspar in successive stage of weathering show the order as follows; feldspar → illite + feldspar → illite + smectite → smectite + kaolinite → kaolinite + silica → kaolinite + gibbsite (Velde, 1985). By the weathering process of Velds, feldspar of rock matrix corresponds to the early or middle stage in the weathering.

Smectite and illite in rock matrix are formed by incongruent dissolution of feldspar according to the following reaction :

$$\text{Plagioclase} + H^+ + Mg^{2+} + H_2O \longrightarrow (Na, Ca)_{0.3}(Al, Mg)_2Si_4O_{10}(OH)_2 \cdot nH_2O + H_4SiO_4 + Na^+ \quad (4)$$

(Smectite)

$$2KAlSi_3O_8 + 2H^+ + H_2O \longrightarrow KAl_2(AlSi_3)O_{10}(OH)_2 + 6SiO_2 + K^+ \quad (5)$$

(K-feldspar) (Illite)

Equation (4) and (5) can be expected in the rock matrix around fracture, where migration of solution can be possible by diffusion. In this condition, alkalies and alkaline earthes are immobile, and thus these cations liberated from feldspar can participate in the formation of smectite and illite in situ. The formation of smectite and illite from feldspars in rock matrix are shown in Fig. 4.

GROUNDWATER CHEMISTRY AND EQUILIBRIUM STATE WITH MINERALS

The five groundwater samples (at 30 m, 50 m, 85 m, 150 m, 185 m in depth) zonally collected from the Surichi borehole are shown to be reducing (available Eh data record values of -54 to -123 mV), alkaline (pH values of 8.6 to 9.2) and sodium bicarbonate waters having Na^+ content of 28.3~42.0 mg/ℓ and HCO_3^- content of 85~

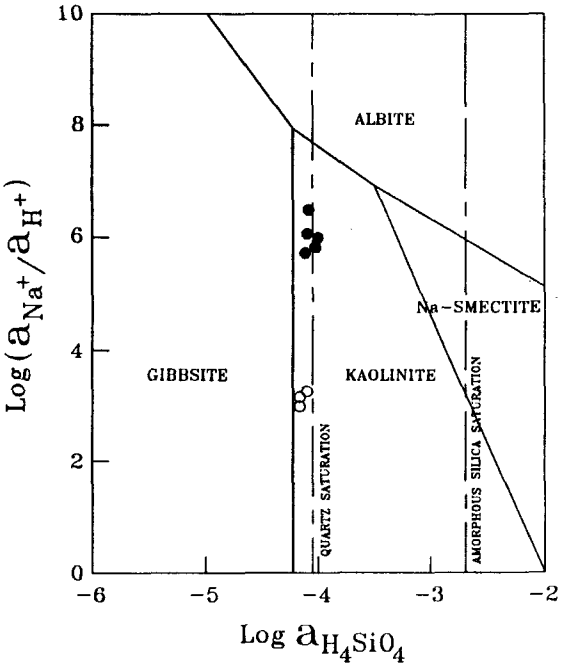

Fig. 9. Mineral stability diagram in terms of Na^+, H^+, and H_4SiO_4 activities in the waters of the Yugu study site. Phase boundaries are after Helgeson, Brown, and Leeper (1969) for water at 25 ℃.

Table 2. Chemical composition of surface water (S) and groundwater (G) from the Yugu study site.

(Unit : mg/ℓ)

Sample No.	Sampling Depth(m)	Cond. (μS/cm)	pH	Eh (mV)	Temp (℃)	Na^+	K^+	Mg^{2+}	Ca^{2+}	HCO_3^-	CO_3^{2-}	SO_4^{2-}	Cl^-	NO_3^-	F^-	E (%)	Si
S1		–	6.86	+33	2.8	3.2	1.1	1.4	2.6	14.0	0.0	3.9	3.7	0.4	0.3	-3.0	4.1
S2		–	7.14	+9	3.1	3.1	1.1	1.6	3.0	12.9	0.0	4.7	4.1	0.2	0.4	-0.4	4.2
S3		–	7.03	+23	4.5	3.2	1.2	1.5	3.3	13.5	0.0	5.4	3.9	2.1	0.2	0.4	4.1
G1	30	146	8.80	-54	11.6	30.1	1.1	1.6	4.8	85.0	1.9	6.4	3.3	0.0	0.7	-0.5	5.5
G2	50	154	8.77	-62	12.0	29.4	1.2	1.2	4.5	86.2	1.9	6.6	3.1	0.02	0.7	1.2	5.5
G3	85	147	8.67	-67	12.1	28.3	0.4	1.3	4.7	78.3	1.4	6.2	3.4	0.02	0.7	-4.2	5.1
G4	150	148	8.83	-104	14.5	36.0	0.5	1.2	4.3	105.0	2.8	6.7	3.3	0.1	0.5	3.4	5.4
G5	185	207	9.20	-123	15.5	42.0	1.5	1.5	4.6	112.0	6.6	6.2	3.8	0.1	0.5	-5.0	5.7

E is the ion balance error expressed in percent.

– :not measured

Table 3. Saturation index(SI) of surface water and groundwater with respect to major minerals, and equilibrium constant of each mineral.

	S-1			S-2			S-3			G-1		
	S.I.	IAP	KT	S.I.	IAP	KT	S.I.	IAP	KT	S.I.	IAP	KT
Albite	-4.11	-22.98	-18.87	-3.81	-22.59	-18.78	-3.87	-22.43	-18.56	-2.33	-21.22	-18.90
Calcite	-3.13	011.54	-8.42	-2.75	-11.18	-8.42	-2.76	-11.19	-8.44	-0.19	-8.61	-8.42
Gibbsite	1.74	10.62	8.88	1.59	10.39	8.80	1.88	10.48	8.60	-0.30	9.20	8.90
Illite	0.27	041.84	-42.11	0.46	-41.46	-41.92	0.69	-40.75	-41.44	-0.52	-42.67	-42.15
Kaolinite	4.28	12.91	8.62	4.09	12.59	8.50	4.43	12.62	8.19	1.62	10.28	8.65
Smectite	1.86	-45.13	-46.99	1.83	-44.97	-46.80	2.11	-44.18	-46.28	-0.43	-47.47	-47.04
Quartz	0.02	-4.17	-4.18	0.06	-4.10	-4.16	-0.05	-4.16	-4.11	0.12	-4.06	-4.19
	G-2			G-3			G-4			G-5		
	S.I.	IAP	KT	S.I.	IAP	KT	S.I.	IAP	KT	S.I.	IAP	KT
Albite	-2.60	-21.47	-18.87	-2.10	-20.96	-18.86	-2.90	-21.61	-18.70	-3.15	-21.77	-18.63
Calcite	-0.22	-8.64	-8.42	-0.33	-8.75	-8.42	-0.08	-8.51	-8.43	0.30	-8.14	-8.43
Gibbsite	0.07	8.94	8.87	0.78	9.64	8.87	-0.30	8.43	8.73	-0.93	7.73	8.66
Illite	-1.12	-43.22	-42.10	0.01	-42.07	-42.08	-2.24	-43.98	-41.74	-3.14	-44.73	-41.59
Kaolinite	1.15	9.76	8.61	2.50	11.10	8.61	0.32	8.71	8.39	-0.99	7.29	8.29
Smectite	-0.99	-47.97	-46.98	0.52	-46.45	-46.96	-1.96	-48.56	-46.60	-3.38	-49.82	-46.44
Quartz	0.12	-4.06	-4.18	0.09	-4.09	-4.18	0.07	-4.08	-4.14	0.04	-4.09	-4.13

112 mg/ℓ. The electrical conductivity of groundwater the range of 146~207 μS/cm. The chemistry of groundwater varies with sampling depth.

The surface waters sampled in the creek nearby the borehole show pH values of 6.86 to 7.14 and very low cations; Na and Ca content of about 3 mg/ℓ, K and Mg of 1~1.5 mg/ℓ, and HCO_3 of 13.0 mg/ℓ, SO_4 and Cl of 3.7~5.4 mg/ℓ. The chemical composition of waters is summarized in Table 2.

The relative proportions of various ions in solution depend on their relative abundances in the rock and their solubility (Fritz et al., 1979). The content of Ca^{2+} and HCO_3^- in groundwater is principally controlled by the calcite-water equilibrium. Weatering of feldspar as well as ion exchange of clay minerals contributes to the sodium content of waters (Tullborg and Larson, 1982). The high sodium content of groundwater is likely to be related to the weathering of albite. This is

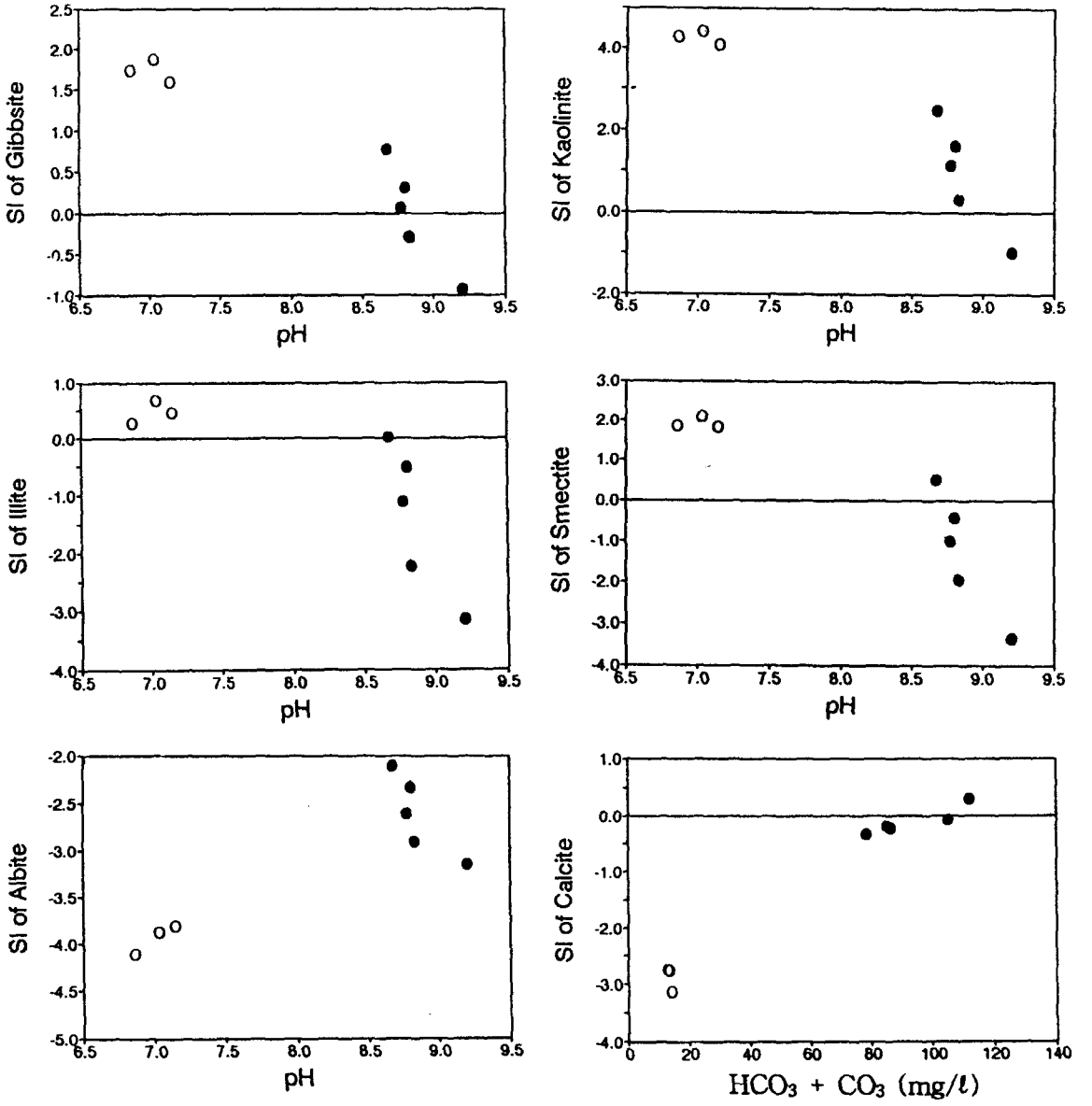

Fig. 10. The diagrams show variation of saturation index of major minerals as a function of pH or bicarbonate and carbonate concentration of waters : open circles are surface water and closed circles are groundwater.

supported by microscopic observation of albite dissolution and negative saturation index of groundwater with respect to albite.

The stability relation of some phases in the Na_2O-Al_2O_3-SiO_2-H_2O system as a function of $[Na^+]/[H^+]$ and $[H_2SiO_4]$ are given by Helgelson et al. (1969). The Surich groundwater and surface water show constant H_2SiO_4 activity. A geochemical evolution of increasing Na^+/decreasing H^+ between surface water and groundwater can be seen on the Helgelson diagram (Fig. 9). In this system kaolinite is stable clay mineral for all waters.

The following ratio is a useful comparision between the status of a mineral dissolution-precipi-

tation reaction at a particular point in time or space and the thermodynamic equilibrium condition ; SI=log IAP/K, where SI is called saturation index (Freeze and Cherry, 1979). The saturation index of mineral phases can be expressed in terms of ion activity product(IAP) and equilibrium constant(K) as follows :

SI=log IAP/K=0 ; Equilibrium state
SI=log IAP/K<0 ; Undersaturation state (mineral dissolution reaction)
SI=log IAP/K>0 ; Supersaturation state (mineral precipitation reaction)

The saturation index of aqueous components with respect to mineral phases were calculated using WATEQ4F computer program, which is based on thermodynamic data. Table 3 shows saturation index and ion activity product of surface water and groundwater with respect to major minerals. The minerals dissolution and precipitation reaction of the groundwater and the surface water are summarized as follows :

(1) Albite is under the dissolution state for all waters, and thus we assume that it is a source mineral for high sodium concentration of groundwater.

(2) The saturation index of calcite show the transition from dissolution state for surface water into equilibrium state for groundwater.

(3) As a function of increaing pH of waters, gibbsite and kaolinite are under precipitation to equilibrium state, and smectite and illite are under equilibrium state to redissolution environment.

Fig. 10 shows the dissolution and precipitation state of clay minerals and albite with the pH variation of waters, and saturation state of calcite based on carbonate and bicarbonate of waters.

CONCLUSIONS

1. The fracture-filling minerals identified from the Surichi borehole in the Yugu site are gibbsite, kaolinite, smectite, illite, calcite, quartz, feldspar, pyrite, chalcopyrite and Fe (or Mn)-oxides.

2. The water-rock interaction in the fractures resulted in the formation of clay minerals by two different processes : (1) Incongruent dissolution of feldspar by groundwater diffused from a fracture path into rock matrix produced smectite and illite in situ. This reaction was restricted to a narrow area along fracture, (2) On the wall of fracture, gibbsite, kaolinite and smectite (or illite) was formed by the precipitation of dissolved species in groundwater. The fracture-filling minerals show the paragenetic sequence of gibbsite, kaolinite and smectite (or illite) in the order. Gibbsite can be formed from $Al(OH)_3$ of soluble Al species liberated from feldspar. Kaolinite was formed by the reaction of $H_4SiO_4+Al(OH)_3$ under the physically and chemically stable environment for a long time. In the late stage of precipitation smecite overgrew on the kaolinite crystals. The evolution of the formation environment of clay minerals was governed by increase of pH due to consumption of hydrogen ions required for the dissolution of feldspar, decrease of fracture permeability by precipitation of kaolinite, and immobility of alkali or alkaline earths in groundwater.

3. The groundwater from the Surichi borehole is a $Na-HCO_3$ type with pH range of 8.6~9.2. The sodium and bicarbonate of groundwater are possibly supplied by the dissolution of albite and calcite, respectively. The secondary clay minerals under the oversaturation state in surface water are now partially redissolved or equilibriated with groundwater throughout precipitation process according to the variation of pH. The stability relation of minerals in the $Na_2O-Al_2O_3-SiO_2-H_2O$ system shows that kaolinite is stable clay mineral for all waters.

ACKNOWLEDGMENTS

This work was carried out by the Radioactive

Waste Management Fund of the Ministry of Science and Technology. The writers thank Dr. C. S. Kim and Dr. S. M. Park for critical reading of this paper.

REFERENCES

Anovitz, L. M., Perkins, D. and Essene, E. J. (1991) Metastability in near-surface rocks of minerals in the system Al_2O_3-SiO_2-H_2O, Clays and Clay Minerals 33, 31-43.

Ball, J. W. and Nordstrom, D. K. (1991) User's manual for WATEQ4F, with revised thermodynamic data base and test cases for calculating speciation of minor, trace and redox elements in natural waters, U. S., Geol. surv., Open File Rep. 91-183, p. 189.

Freeze, R. A. and Cherry, J. A. (1979) Groundwater, Prentice-Hall, Inc., p. 604.

Fritz, P., Barker, J. f., and Gale, J. E. (1979) Geochemistry and isotope hydrology of groundwaters in the Stripa granite : results and preliminary interpretation, LBL 1152, Lawrence Berkeley Laboratory, p. 135.

Helgeson, H. C., Brown, T. U., and Leeper, R. H. (1969) Handbook of theoretical activity diagrams depicting chemical equilibria in geological systems involving an aquous phase at one atm. and 0° to 300 ℃ San Francisco : Freeman, Copper and Co., p. 253.

Huang, W. H. and Keller, W. D. (1973) Gibbs free energies of formation calculated from diverse environments of origin-Ⅳ. Georgia kaolin and kaolinizing source rocks : Clays and Clay Minerals. 25, 311-345.

Muller, J. P., Clozel, B., Idefonse, P. and Calas, G. (1992) Radiation-induced defects in kaolinites : indirect assessment of radionuclide migration in the geosphere, Applied Geochemistry, Suppl. Issue No. 1, 205-216.

Nriagu, J. O. (1975) Thermochemcial approximation for clay minerals, American Mineralogist, 60, 834-839.

Sasowsky, I. D. and White, W. B. (1993) Geochemistry of the Obey river basin, Northcentral Tennessee : a case of acid mine water in Karst drainage system, Jour. of Hydrology, 146, 29-48.

So, C. S., Shelton K. L. Chi, S. J. and Choi, S. H. (1988) Stable isotope and fluid inclusion studies of gold-silver-bearing hydrothermal-vein deposits, Cheonan-Cheongyang-Nonsan mining district, Republic of Korea : Cheongyang area, Jour. Korean Ins. Mining Geology, 21, 149-164.

Tullborg, E. L. and Larson, S. A. (1982) Fissure filling from Finnsjon and Studsvik, Sweden-Identification, Chemistry and Dating, SKB 82-20, p. 76.

Tullborg, E. L. and Larson, S. A. (1983) Fissure fillings from Gidea, central Sweden, SKB-TR 83-12, 83-74.

Tullborg, E. L. (1986) Fissure filling from Klipperas study site, SKB-TR 86-10, p. 72.

Velde, B. (1985) Clay minerals. A physics-chemical explanation of their occurrence, Dev. in sedimentology 40, Elsevier, Amsterdam, p. 427.

Woods, T. L. and Garrels, R. M. (1987) Thermodynamic values at low temperature for natural inorganic materials : An uncritical summary, Oxford university press, New York, p. 242.